Proceedings of the 1991 IEEE
International Conference on Robotics and Automation
Sacramento, California - April 1991

PATH PLANNING FOR SPACE MANIPULATORS TO MINIMIZE SPACECRAFT ATTITUDE DISTURBANCES

Steven Dubowsky
Miguel A. Torres

Department of Mechanical Engineering
Massachusetts Institute of Technology
Cambridge MA 02139

Abstract

A technique called the Enhanced Disturbance Map to plan space manipulator motions that will result in relatively low spacecraft disturbances is presented. Although a spacecraft's attitude control reaction jets can compensate for the dynamic disturbances imposed on its spacecraft by its manipulator's motions, reaction jet fuel is a limited resource. Excessive disturbances would limit the life of a system. The Enhanced Disturbance Map can aid in understanding this complex problem and in the development of algorithms to reduce disturbances, including ones that use manipulator redundancy to eliminate the disturbances.

1. Introduction

Telerobotic manipulator systems have been proposed as an alternative to costly and hazardous Extra Vehicular Activity (EVA) [1]. However, the development of such robotic systems creates a number of technical challenges, including those in the dynamics and controls area [2]. Many of these control problems result from the dynamic disturbances to the system's spacecraft attitude and position caused by its manipulator's motions. Although these spacecraft motions can be controlled using the system's attitude control reaction jets, this could require substantial amounts of attitude control fuel, limiting the useful "on orbit" life of the system [3]. To minimize the dynamic disturbances acting on the spacecraft, and hence enhance a system's life, planning algorithms employing numerical optimization techniques have been proposed [4,5]. Unfortunately these techniques, like most numerical optimizations of nonlinear problems, can require excessive amounts of computational effort for realistic systems, and cannot guarantee global optimal solutions. They also fail to provide insights into the structure of the problem that can aid the system planner in finding the best solution.

The Virtual Manipulator (VM) has been used to develop a tool called the Disturbance Map which improves the understanding of the dynamic disturbance problem by showing, graphically, directions of the manipulator's motion in joint space which result in maximum and minimum dynamic disturbances to the spacecraft [6,7]. It was suggested that the DM could be used for planning the paths of manipulators so as to reduce manipulator motion-caused dynamic disturbances to its spacecraft attitude. However, in its original form, the DM was not an effective tool for this purpose. The Fixed-Attitude Restricted Jacobian or the FAR-Jacobian has also been proposed as a method to find manipulator paths which result in reduced attitude disturbances to a free-floating spacecraft [8].

This paper presents an improved form of the DM called the Enhanced Disturbance Map (EDM) and shows how it can be effectively used to plan manipulator motions to reduce these disturbances. Reducing manipulator-caused disturbances reduces the need for a space manipulator system to carry large amounts of costly attitude fuel. The paths found using the EDM can be used either directly or as "good" starting solutions for numerical optimization methods in order to decrease computational effort and increase the likelihood that such solutions will converge to the globally optimal ones. Also, a method is presented for efficiently calculating the EDM of manipulators with more than two Degrees-of-Freedom (DOF). The original DM was applied only to two-link planar manipulator systems.

Three methods that use the EDM are proposed to suggest paths for a given manipulator which result in low attitude fuel consumption. The first uses the EDM to position and orient a spacecraft so that a zero dynamic disturbance path can be found between given end-point positions in inertial space. The second selects reduced disturbance paths by avoiding regions in a manipulator's joint space where small manipulator motions cause large disturbances to the spacecraft: this method is termed the "Hot Spot" approach. Finally, the third method uses the EDM to find zero disturbance paths for redundant manipulators

2. System Dynamic Model

Consider a system with an n DOF rigid manipulator mounted on a rigid spacecraft, see Fig. 1. The spacecraft has six-DOF, three positions and three orientations in inertial space. The six coordinates used to represent the spacecraft position and orientation are the inertial position of its centroid expressed in body fixed axes, $\mathbf{X_b} = [x, y, z]^T$, and its orientation in terms of Roll, Pitch and Yaw angles expressed also in body fixed axes, $\Theta_b = [\phi, \theta, \psi]^T$.

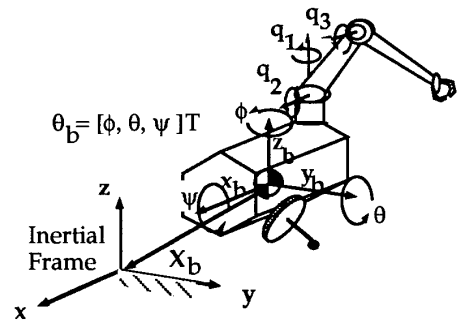

Fig. 1. System Generalized Coordinates.

A set of n coordinates is required to describe the configuration of the n DOF manipulator. These coordinates are chosen to be the relative manipulator joint displacements, $\mathbf{q} = [q_1, q_2, \ldots, q_n]^T$, see Fig. 1. The generalized coordinates used to write the dynamics of the system are the elements of the vector ξ, where ξ is $[\mathbf{X_b}, \Theta_b, \mathbf{q}]^T$. The generalized force vector is defined as $\boldsymbol{F} = [f_x, f_\theta, f_q]^T$, where f_x and f_θ are three-element vectors composed of the external forces and torques produced by the system's reaction jets expressed in the body-fixed frame and acting on the centroid of the spacecraft. The elements of the vector f_q are the torques produced by the n manipulator joints. The system equation of motion can then be written as:

$$\mathbf{H}(\xi)\ddot{\xi} + \mathbf{C}(\xi,\dot{\xi})\dot{\xi} = \mathbf{F} \qquad (1)$$

where $\mathbf{H}(\xi)$ is an n+6 by n+6 symmetric, positive definite inertia matrix, $\mathbf{C}(\xi,\dot{\xi})$ is an n+6 by n+6 matrix due to centrifugal and Coriolis effects, and $\boldsymbol{F}$ is the n+6 element generalized force vector.

The system generalized momentum vector, π, is:

$$\mathbf{H}(\xi)\dot{\xi} = \pi \qquad (2)$$

The elements of π are $\pi_x, \pi_y, \pi_z, \pi_\phi, \pi_\theta, \pi_\psi, \pi_1, \pi_2, \ldots$ and π_n, π_x, π_y, and π_z are the x, y, z components of the linear momentum of the center of mass of the spacecraft; and π_ϕ, π_θ, and π_ψ are the components of the angular momentum of the spacecraft. All are measured with respect to the spacecraft fixed axes. The components $\pi_1, \pi_2, \ldots$, and π_n represent the momentum in the direction of each of the manipulator's respective joint axes.

Eq. 2 is used to develop an algorithm for computing the disturbance maps. Eq. 1 is the basis of a simulation used to model the dynamic performance of space manipulators, including their spacecraft and control systems [3]. It is used in this study to evaluate the effectiveness of the disturbance map-based planning algorithms.

3. The Disturbance Map

3.1. The Original Formulation

Infinitesimal changes in spacecraft attitude, $\delta\Theta$, can be expressed as a function of infinitesimal manipulator joint motions, $\delta\mathbf{q}$, as $\delta\Theta = \mathbf{G}'(\mathbf{q},\Theta)\delta\mathbf{q}$, where $\mathbf{G}'$ is a 3 by n disturbance sensitivity matrix [6,7]. If the spacecraft's angular motions are measured with respect to the spacecraft's body-fixed axes described above, then $\mathbf{G}'$ becomes $\mathbf{G}$, which is only a function of the joint variable vector, $\mathbf{q}$. The following equation can be written:

$$\delta\Theta_b = \mathbf{G}(\mathbf{q})\delta\mathbf{q} \qquad (3)$$

The vector $\delta\Theta_b$ is defined as the instantaneous disturbance. Singular value decomposition of $\mathbf{G}$ gives the directions and magnitudes of the maximum and minimum spacecraft disturbances as a function of $\mathbf{q}$ [9]. References [6-7] show that for a two-link planar manipulator the directions of the minimum and maximum disturbances are orthogonal in joint space, and that the magnitude of the minimum disturbance is zero at all points in this space. Plotting these maximum disturbances and the directions of the minimum disturbances at a finite number of points in the two-dimensional joint space results in the original form of the DM, shown in Fig. 2.

At each point $\mathbf{q} = [q_1, q_2]^T$ in this map, the magnitude of the maximum disturbance is represented by the length of the arrow. The DM is only dependent on the dynamic and kinematic parameters of the system: i.e., the body masses, inertia tensors, and dimensions. The inertial position and orientation of the spacecraft does not affect the DM's shape if Θ_b is measured with respect to the spacecraft. This makes the Disturbance Map a suitable tool for visualizing the dynamic behavior of space manipulators based exclusively on their dynamic and kinematics parameters. However, this form makes it difficult to visualize low disturbance paths and it is impractical to apply to manipulators with more than two links. An effort to improve these aspects of the DM led to the development of the more effective form of the map discussed in this paper.

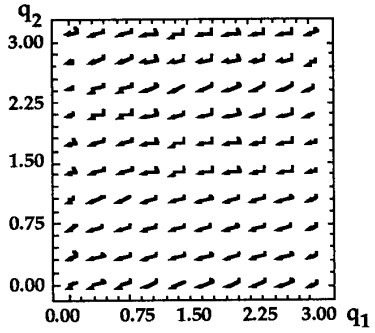

Fig. 2. The Original Disturbance Map.

3.2. Computing The Disturbance Map

References [6-7] present a method for computing the disturbance map for a two DOF manipulator by using the Virtual Manipulator. Here a method for efficiently computing the map for manipulators with more than two DOF is given. Eq. 2 defines a generalized momentum vector π based on the selected generalized coordinates described above. The inertia tensor of Eq. 1 can be written as:

$$\mathbf{H}(\xi) = \begin{bmatrix} \mathbf{A} & \mathbf{B} \\ \mathbf{C} & \mathbf{D} \end{bmatrix} \qquad (4)$$

where $\mathbf{A}$ is a 6 by 6 symmetric submatrix relating the linear and angular velocity vectors of the spacecraft to its linear and angular momentum, $\mathbf{B}$ is a 6 by n mass matrix relating the motion of the joints to the spacecraft linear and angular momentum, and $\mathbf{C}$ equals $\mathbf{B}^T$ [3]. The $\mathbf{D}$ is an n by n matrix relating the joint velocities to their momenta. It is not used in calculating the DM.

Assuming that the system is at rest and no external forces or torques act upon it, Eq. 2 becomes:

$$\mathbf{H}(\xi)\dot{\xi} = \mathbf{0} \qquad (5)$$

A discussion of the above assumption is contained in Section 3.4. Now, using Eq. 4 and recalling that ξ is $[\mathbf{X_b}, \Theta_b, \mathbf{q}]^T$, Eq. 6 is solved for $[\dot{\mathbf{X}}_b, \dot{\Theta}_b]^T$ to yield:

$$[\dot{X}_b^T, \dot{\Theta}_b^T]^T = -A^{-1}B\,\dot{q} \qquad (6)$$

By replacing the derivative operation by a variation, letting $Z = [z_1, z_2]^T = -A^{-1}B$, and noting that that z_1 and z_2 are 3 by n matrices, Eq. 6 becomes:

$$\begin{bmatrix}\delta X \\ \delta\Theta_b\end{bmatrix} = \begin{bmatrix}z_1 \\ z_2\end{bmatrix}\delta q \qquad (7)$$

The goal of the algorithm is to find the relationship between the changes in orientation of the base $\delta\Theta_b$ and motion of the manipulator joints δq. This is obtained from Eq. 7 as $\delta\Theta_b = z_2\,\delta q$. This expression is the same as Eq. 3 required for the Disturbance Map, so G is z_2. The matrix z_2 is a submatrix of $H(x)$, which is computed quite efficiently by the modified Walker and Orin algorithm, developed in this study to treat manipulators with moving bases [3]. Finally, a singular value decomposition of the matrix z_2 gives the directions and magnitudes of maximum and minimum disturbances required for plotting the Disturbance Map [9].

3.2 The Enhanced Disturbance Map

The Enhanced Disturbance Map derives from studying the attitude disturbances to a system's spacecraft by its manipulator at an arbitrary point in the manipulator's joint space. Consider the disturbance for a two DOF manipulator at some point in its joint space, such as shown in Fig. 3a. References [6-7] show that for all such points there are directions of maximum and minimum disturbances and moreover that these directions are perpendicular to each other. The magnitude of the disturbance varies in a dipole fashion as shown in Fig. 3a [3].

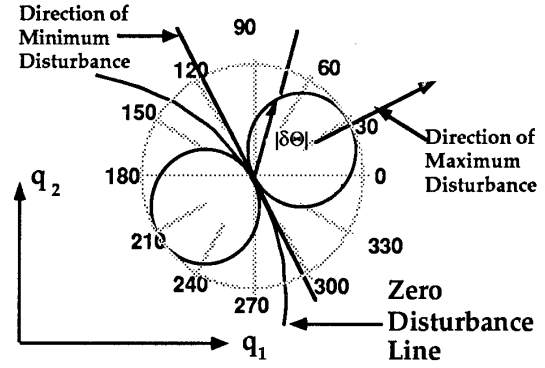

a. A Two DOF Manipulator.

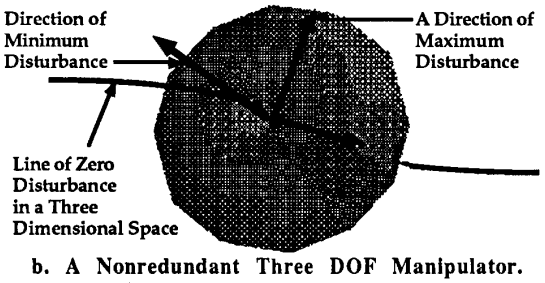

b. A Nonredundant Three DOF Manipulator.

Fig. 3. Locus of the Disturbance Magnitude at a Manipulator's Disturbance Map Point.

Fig. 3.b shows the disturbance characteristics of the three-link spatial manipulator with two parallel axes, such as shown in Fig. 1. Here, too, there exists a direction in joint space for which small manipulator motions do not disturb the spacecraft attitude. In a redundant system there may be more than one direction of zero disturbance.

The existence of these local zero disturbance directions suggest that paths constructed to lie largely along the lines of zero disturbance will result in low fuel usage. Motions across or perpendicular to a zero disturbance line will result in a local maximum spacecraft disturbance, or high fuel consumption. The original Disturbance Map was recast to show the lines of zero disturbance, such as shown in Fig. 4. This new form is called the Enhanced Disturbance Map; it permits the representation of three DOF manipulators on graphics computer terminals. The magnitudes of the maximum disturbances are shown by coloring the lines proportional to the maximum disturbance magnitude at that point. This coloring makes obvious high and low maximum disturbance areas, called "hot spot"and "cool spots", respectively. It is not possible to reproduce the colors in the figures of this paper, and therefore, where needed, they are represented by background shading.

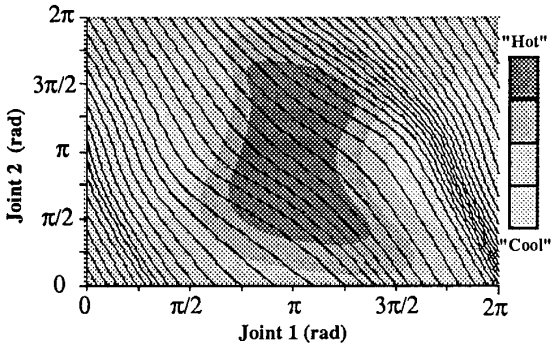

Fig. 4. The Enhanced Disturbance Map.

3.4. Attitude Disturbances, Fuel Consumption and The Enhanced Disturbance Map.

Future space manipulator system spacecraft are likely to be equipped with reaction jets, reaction wheels, or both. Reaction jets can control both system attitude and the position. However, jet fuel in space is limited. Reaction wheels, which can be powered by renewable solar energy, can only control a system's attitude and can be easily saturated by large rotational disturbances. As discussed below, systems using either or both of these spacecraft control techniques can benefit from the use of the EDM in planning the motions of their manipulators.

The amount of instantaneous power required from a system's reaction wheels to compensate for the rotational disturbances produced by its manipulator's motion can be shown to be directly proportional to the instantaneous rotational disturbance, given by Eq. 3 and plotted in the disturbance maps. So, for example, systems with manipulators whose paths follow zero disturbance lines in the EDM would avoid reaction wheel saturation problems. The reaction jet fuel required to correct a spacecraft's position and attitude in the presence of manipulator motion disturbances is not as simple. It can be shown

that the fuel used to hold a spacecraft stationary during a manipulator's maneuver varies directly as the level of dynamic disturbance to spacecraft [3]. These disturbances are a function of the path taken by the manipulator and of the velocity of the manipulator's motion along that path. Generally, the faster the motion, the more fuel is used. This study does not consider the issue of the dependence of the fuel usage on manipulator speed because we assume that if a manipulator path is found which results in relatively low disturbance to the spacecraft, then relatively low fuel usage results. These low disturbance paths can be used directly where the manipulator velocity profile is determined by other considerations, or as initial paths for numerical optimization procedures which include the effects of manipulator speed.

Disturbance to the spacecraft consists of translational and rotational components. Reaction jets would need to compensate for the translational component if translations of the spacecraft are undesirable. Rotational disturbance must be overcome to eliminate spacecraft attitude changes. The total rotational disturbance is defined to be the integral of the absolute value of the instantaneous dynamic disturbances, $|\delta\Theta_b|$, along the manipulator path [3]. The fuel consumption due to linear disturbances has been shown in simulations, at least for the systems considered in this system, to be smaller than that due to the rotational disturbance. If the translational disturbance is uncontrolled during a manipulator motion between given end-points, it can also be shown that the total translational shift of the spacecraft is not a function of the manipulator's path between those points [6]. Hence, we assumed that the fuel required to hold the linear location of the system stationary is not a strong function of the manipulator paths for relatively smooth paths. Therefore, this study focuses on developing methods that would minimize both the instantaneous rotational disturbance to the spacecraft to prevent saturation of reaction wheels and the total rotational disturbance to minimize reaction jet fuel usage.

Note that the mass properties of the system are assumed to be constant in the above development of the equations used to generate the EDM. If the system grasped a payload at some point the map would need to be recalculated. Generally, however, such an action would not be planned to occur when the manipulator is undergoing large motions which could disturb the spacecraft. It should also be noted that the derivation of the equations assumes that the linear and angular moment of the system, π, is zero with respect to some Newtonian frame of reference, see Eq. 2. Usually, however, a manipulator system would not be expected to perform tasks while it is tumbling or while its center of mass is experiencing a substantial change in linear velocity. If these conditions are met, and reaction wheels are used, then the underlying assumptions of the map's development are satisfied. Since reaction jets will change the system's linear and angular momentum, and hence, the conditions may not be rigorously met at all times. However, if the purpose of the reaction jet system is to hold the spacecraft's position and attitude constant and the initial and final velocities of the manipulator are zero, the method should yield a good approximation to the true disturbance map and useful results. This has been our experience with the techniques and is shown in the examples presented in this paper.

4. Techniques for Minimizing Fuel

Three methods are discussed below for using the EDM to suggest paths which result in less attitude fuel consumption. First, the EDM is used to position and orient the spacecraft so that a zero dynamic disturbance path can be found. Second, paths are selected which avoid regions where small motions of the manipulator cause large disturbances to the spacecraft. Finally, the EDM is used to find zero disturbance paths for redundant manipulators. The simple system shown in Fig. 5 is used in the first two examples presented. Each of its bodies has a mass of 100.0 kg, an inertia of 10 kg-m-m.

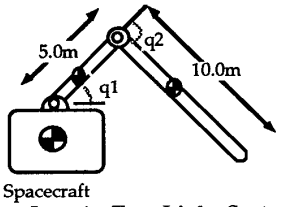

Fig. 5. A Two-Link System.

4.1. Spacecraft Relocation

It is always possible, given the initial and final end points of a motion in inertial space to relocate the spacecraft position and orientation for planar systems so that a manipulator path exists which results in zero angular spacecraft disturbance [3]. Such a path will be achieved if the initial and final positions of the manipulator lie on the same zero disturbance line in the EDM, and if the manipulator follows that zero disturbance line from the initial point to the final position. Algorithms to find such paths can be developed by noting that the initial and final EDM positions of the manipulator for given inertial end-effector positions depend on the position and orientation of the spacecraft. One such algorithm developed here first finds the manipulator EDM position for the system, given the system's initial end-effector position and some arbitrary spacecraft position and orientation. Then the zero disturbance line passing through this EDM point is computed. Next, the system is rotated about this initial end-effector position in inertial space by some angle. Note that the EDM does not change because it shows the disturbances with respect to the spacecraft axes. This rotation changes the EDM's final position of the manipulator without changing the EDM position of the initial path point. The algorithm then determines the rotation angle required for the final EDM position to be on the same zero disturbance line that passes through the initial position. This algorithm is described in detail in Reference [3].

In the following example, the objective is to move the manipulator end-point, shown in Fig. 6, from an initial point in inertial space, point I, to a final point, point F. An arbitrary spacecraft location and an arbitrary path from point I to point F is shown in Fig. 6a. This path is shown in the Disturbance Map in Fig. 7, as the line from I to F, where it runs almost perpendicular to the EDM zero disturbance lines. Simulations show that this path results in the use of substantial reaction jet control fuel to hold the spacecraft completely stationary. But by using the algorithm described above a new position and orientation of the spacecraft was calculated, see Fig. 6b. The final con-

figuration of the base was rotated by 63.03 degrees counterclockwise around the end-effector initial position. This placed the final point, called F', on the same zero disturbance line as the initial point, see Fig. 7. Using the zero disturbance line I to F' as the path, the rotational disturbances are zero; hence the fuel usage, is essentially zero.

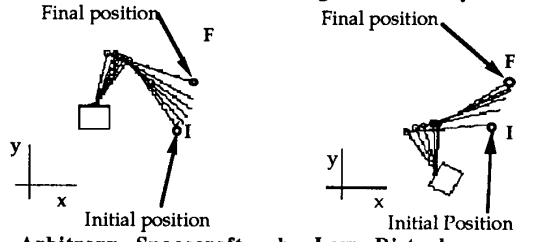

a. Arbitrary Spacecraft Position. b. Low Disturbance Spacecraft Position.

Fig. 6. Inertial Motions of a System Before and After Spacecraft Relocation.

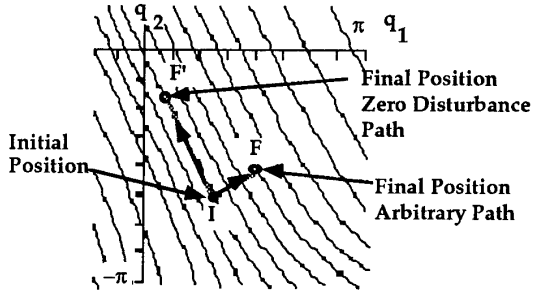

Fig. 7. Initial and Final Configurations Before and After Reorienting the Spacecraft.

This approach is most appropriate where the manipulator will be making a series of nearly repetitive moves because of the reaction jet fuel required to reposition the spacecraft.

4.2. The "Hot Spot" Method

Another method to minimize fuel consumption based on the Enhanced Disturbance Map is the "Hot Spot" method which is useful in cases where it is not practical to reposition the spacecraft, including those occasions when interference with other objects may result.

Consider the case where the initial and final manipulator end-points are fixed in inertial space. These points are also fixed in the EDM, assuming the attitude control system keeps the spacecraft stationary during the manipulator's motion. Fig. 8a shows a two-link space manipulator and its EDM with pseudo coloring, and a straight line path between the assumed initial and final points, points I and F, respectively. As the manipulator moves its end-point from I to F in inertial space, its joint angles will move between the corresponding points I and F shown in the Enhanced Disturbance Maps, also contained in Fig. 8a. The dark areas of the EDM, shown in Fig. 8a represent "hot spots", or areas of higher maximum dynamic disturbance. Notice that the initial configuration or point I in this example lies in a "hot spot". This path would produce substantial rotational disturbances to the spacecraft. Thus, the "Hot Spot" approach is: if a path must go through EDM regions of large disturbance, then it should follow the zero disturbance lines as closely as possible. When disturbances are low, at "Cool Spots", the path may move across disturbance lines. Three paths were considered following this rule for the system shown in Fig. 8 in order to show the effectiveness of this approach. The first is the straight line from I to F, shown in Fig. 8a. The second is contoured to follow the zero disturbance line in the "hot" region shown in Fig. 8b; the third moves across the zero disturbance lines in the "hot region" shown in Fig. 8c.

The total reaction jet fuel required to hold the spacecraft stationary in each of the three case was computed using the simulation programs described earlier, and are shown in Fig. 9. Recall that fuel usage is a function of the velocity profile of a manipulator along its path, as well as the shape of the path in the EDM. The same velocity profile was used in each case in this example. The manipulator started from rest at point I and moved with a constant acceleration until midway along the path; it then used the same constant deceleration to come to a stop at position at F. All these movements were completed in 1.0 seconds.

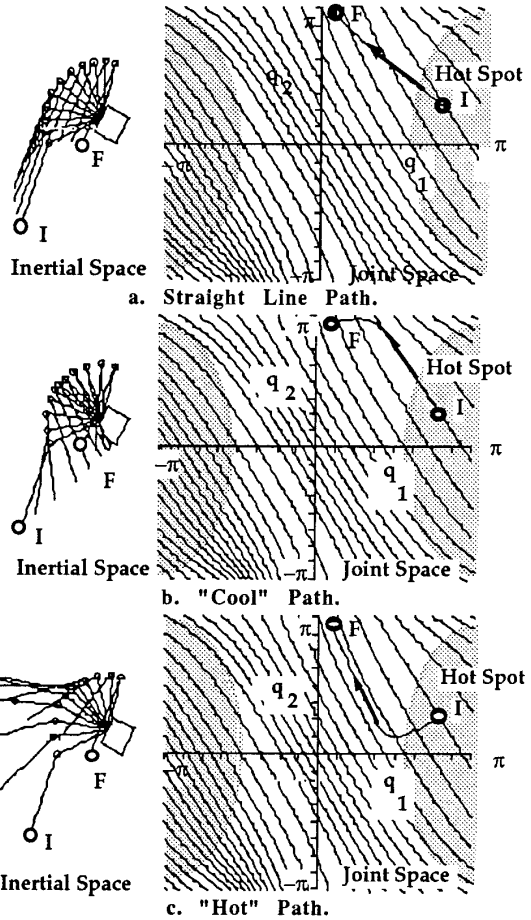

Fig. 8. "Hot Spot" Path Selection.

Fig. 9 clearly shows that the path selected by the "Hot Spot" approach, shown in Fig. 8b, reduces the amount of fuel below level of the simple straight line path; moving

across the disturbance lines in high disturbance regions, such as shown in Fig. 8c, increases fuel consumption. Fig. 9 also shows that the fuel required to compensate for the translational disturbances is less than that required for the rotational disturbances, except in the case where the rotational fuel has been optimized by the Enhanced Disturbance Map. Furthermore, while the amount of position fuel varies from path to path, it is not a strong function of the path used.

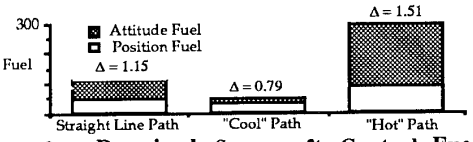

Fig. 9. Required Spacecraft Control Fuel.

A measure of the angular disturbance, called Δ (radians), produced by manipulator motion was computed for each of the paths as the integral over the path of the magnitudes of the disturbance, $|\delta\Theta_b|$. The values of Δ for each path are shown in Fig. 9. It can be seen that this simply computed measure agrees well with actual fuel usage.

4.3. Minimizing Fuel in Redundant Systems

The EDM has led to an algorithm to reduce fuel consumption in systems with redundant manipulators. Consider the three-link redundant manipulator moving in a planar space from point I to F, with its spacecraft held stationary by its control system (see Fig. 10).

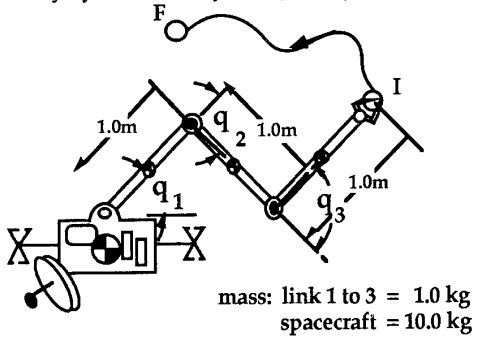

Fig. 10. A Redundant Planar Manipulator.

The form of the Enhanced Disturbance Map for such a three DOF redundant manipulator is shown in Fig. 11. The EDM will be a three dimensional space, whose axes are the three manipulator joint variables. For this redundant manipulator, the directions of zero angular dynamic disturbance motion can be represented as a two dimensional manifold or surface in joint space rather than as lines, as for nonredundant manipulators.

Given the initial position of system, called point I in Fig. 11, the zero disturbance surface passing through this point can be found by the direct application of the above equations and singular value decomposition. Next, it is noted that, because the manipulator is redundant, the final position of the end-effector in inertial space, F, maps into a locus of points, a curved line, in joint space, as shown in Fig. 11. If the value of F in joint space is chosen as the intersection of the zero disturbance surface and this locus, and if the path from I to this point is chosen to lie in the zero disturbance surface, then manipulator motion will not result in any angular disturbances to the spacecraft. This path is called **S(q)** and can be computed relatively easily [3]. It should be noted that this algorithm works equally as well for nonplanar redundant systems.

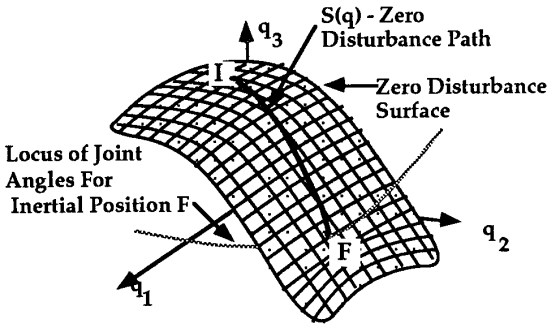

Fig. 11. The Zero Disturbance Manifold of a Three DOF Redundant Manipulator.

The following is an example of the results from using this method. The computed paths are simulated with the system's reaction jets on, in order to prevent the spacecraft from moving, and the fuel required for each path is computed. Fig. 12a shows the manipulator of Fig. 10 at an initial end effector position, I. Its corresponding position in three dimensional joint space is shown in Fig. 13. The zero disturbance surface passing through point I in joint space is also shown in two views in Fig. 13. Fig. 13 also shows an arbitrary path from point I to point F; F corresponds to just one of the infinite configurations which locate the end-effector at F in inertial space. Notice from the back view in Fig. 13 that this path does not stay on the zero disturbance surface passing through I.

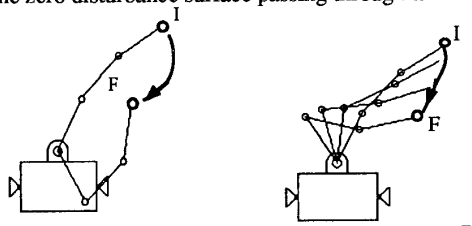

a. Arbitrary Path. b. Zero Disturbance Path.

Fig. 12. Two Redundant Manipulator Paths With The Same Inertial Space End-points.

Fig. 14 shows a path that has been computed to move the manipulator's end-effector from the same points I to F in inertial space while staying on the zero disturbance surface passing through I. This path is shown in Fig. 12b.

The motions along the two paths were simulated allowing reaction jets to compensate for any dynamic disturbance, and the fuel usage was recorded. The velocity profile along the path was chosen to be a half sinusoidal wave with initial and final velocities equal to zero. The magnitudes of the maximum velocity, which varies with the length of the path, was computed so that all maneuvers would take 2 seconds. For the arbitrary path, the total angular and linear fuel required was 0.587 units of fuel. The zero disturbance path required only 0.160 units, a substantial reduction. This zero disturbance path fuel was required mostly to compensate for translational disturbances to the spacecraft.

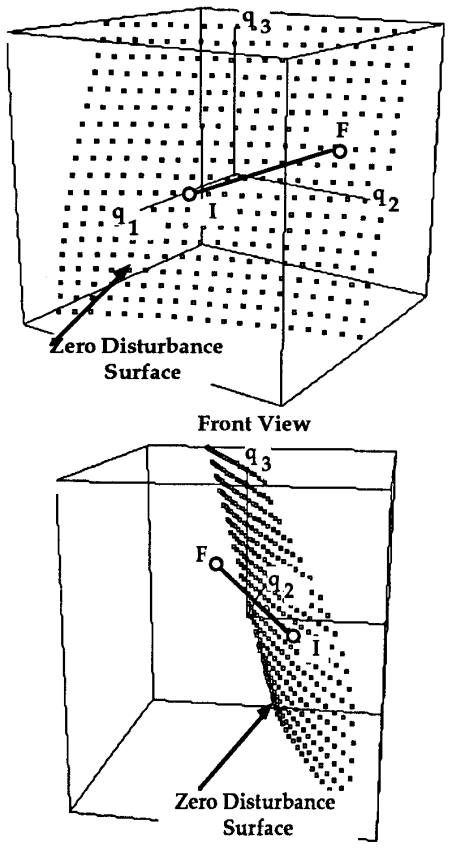

Fig. 13. Redundant Space Manipulator Arbitrary Path Maneuver.

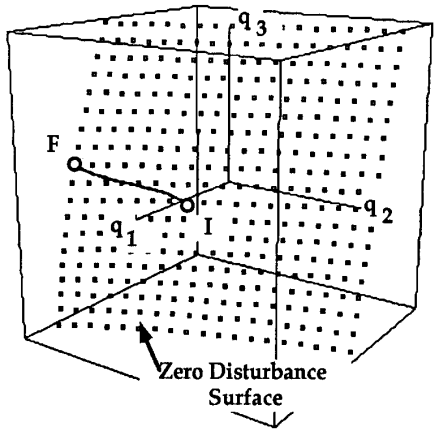

Fig. 14. Redundant Space Manipulator Computed Path Maneuver.

In this study several other algorithms were developed using the EDM to shape manipulator paths to reduce the disturbances to the spacecraft. A description of these methods are beyond the scope of this paper and the reader is referred to reference [3].

5. Conclusions

The Enhanced Disturbance Map has been shown to aid in understanding the problem of dynamic disturbances to spacecraft caused by manipulator motion in space robotic systems and in finding paths to minimize such disturbances. While the EDM and its zero disturbance lines or surfaces can only be displayed for three DOF manipulators using modern computer graphics terminals, computer algorithms can be developed that trace their way through the multi-dimensional joint space of higher order systems by using the understanding given by the 3-D disturbance maps. For example, this paper shows the Enhanced Disturbance Map can be used to demonstrate the existence of zero disturbance paths for redundant space manipulators and to develop an algorithm to find such paths. That algorithm is valid for general spatial manipulators with more than six DOF.

The EDM also can be used to obtain near-optimal paths which minimize these dynamic disturbances. These paths can be used directly, or as "good" starting solutions for numerical optimization methods; they decrease the computational effort for such methods and increase the likelihood that they will converge to true global optimal solutions.

6. Acknowledgements

The support of this work by NASA (Langley Research Center, Automation Branch) under Grant NAG-1-801 and M. Torres NASA fellowship is acknowledged.

7. References

1. Bronez, M.A., Clarke, M.M., and Quinn, A., "Requirements Development for a Free-Flying Robot - The 'ROBIN'," Proc. 1986 IEEE Inter. Conf. on Robotics and Auto., April 7-10, 1986, San Francisco, CA, pp. 667-672.

2. Proc. of NASA Conf. on Space Telerobotics, Jan. 31-Feb.2, 1989, Pasadena, CA.

3. Torres, M., "The Disturbance Map and Minimization of Fuel Consumption During Space Manipulator Maneuvers," MS Thesis, Depart. of Mech. Engr., MIT, 1989, Cambridge, MA.

4. de Silva, C.W., Chung, C.L., and Lawrence, C., "Base Reaction Optimization of Robotic Manipulators for Space Applications," Proc. Inter. Symposium of Robots, Sydney, Australia, Nov. 1988.

5. Quinn, R.D., Chen, J.L., and Lawrence, C., "Redundant Manipulators for Momentum Compensation in Micro-Gravity Environment," Proc. AIAA Guidance, Navigation and Control Conf., New York, 1988, pp. 581-587.

6. Vafa, Z., and Dubowsky, S., "On the Dynamics of Manipulators in Space Using the Virtual Manipulator Approach," Proc. 1987 IEEE Inter. Conf. on Robotics and Auto., March 30-April 3, 1987, Raleigh, NC.

7. Vafa, Z. and Dubowsky, S., "On the Dynamics of Space Manipulators Using the Virtual Manipulator, with Applications to Path Planning," J of the Astronautical Sciences, Special Issue on Space Robotics, Vol. 38, No. 4, Oct.-Dec. 1990, pp. 441-472.

8. Nenchev, D., Yoshida, K., and Umetani, Y., "Analysis, Design and Control of Free-Flying Space Robots Using Fixed-Attitude-Restricted Jacobian Matrix", Fifth Inter. Sym. on Robotic Res., Aug. 28-31, 1989, Tokyo, Japan, pp. 251-258.

9. Strang, G., Introduction to Applied Mathematics, Wellesley-Cambridge Press, Wellesley, MA, 1986.